Physics Letters B 842 (2023) 137944

Contents lists available at ScienceDirect

Physics Letters B

journal homepage: www.elsevier.com/locate/physletb

Four-loop splitting functions in QCD – The quark-quark case

G. Falcioni [a], F. Herzog [a], S. Moch [b,*], A. Vogt [c]

[a] Higgs Centre for Theoretical Physics, School of Physics and Astronomy, The University of Edinburgh, Edinburgh EH9 3FD, Scotland, UK
[b] II. Institute for Theoretical Physics, Hamburg University, Luruper Chaussee 149, D-22761 Hamburg, Germany
[c] Department of Mathematical Sciences, University of Liverpool, Liverpool L69 3BX, UK

ARTICLE INFO

Article history:
Received 24 February 2023
Accepted 29 April 2023
Available online 11 May 2023
Editor: A. Ringwald

ABSTRACT

We have computed the even-N moments $N \leq 20$ of the pure-singlet quark splitting function $P_{\rm ps}$ at the fourth order of perturbative QCD via the anomalous dimensions of off-shell flavour-singlet operator matrix elements. Our results, derived analytically for a general gauge group, agree with all results obtained for this function so far, in particular with the lowest six even moments obtained via physical cross sections. Using these results and all available endpoint constraints, we construct approximations for $P_{\rm ps}$ at four loops that should be sufficient for most collider-physics applications. Together with the known results for the non-singlet splitting function $P_{\rm ns}^+$ at this order, this effectively completes the quark-quark contribution for the evolution of parton distribution at N^{3}LO accuracy. Our new results thus provide a major step towards fully consistent N^{3}LO calculations at the LHC and the reduction of the residual uncertainty in the parton evolution to the percent level.

Collinear factorization in Quantum Chromodynamics (QCD) is controlled by a set of universal functions, the splitting functions P, governing the scale dependence of the parton distribution functions (PDFs), which are essential ingredients in all theoretical predictions for scattering processes with initial-state hadrons [1]. The splitting functions are calculable in the perturbative approach to QCD. They have been known, for a long time, at three-loop accuracy [2,3], which is the next-to-next-to-leading order (NNLO or N^{2}LO) in the expansion in powers of the strong coupling $\alpha_{\rm s}$.

This theoretical accuracy, however, faces challenges due to the precision of the currently available experimental data collected at the Large Hadron Collider (LHC). Also, the expectations for the LHC's Run 3, the high-luminosity phase (HL-LHC) as well as the plans for the future Electron-Ion Collider (EIC) [4] indicate the need to increase the precision by one quantum loop to N^{3}LO accuracy. This will reduce the uncertainty in the parton evolution to percent-level precision. It is also required for a fully consistent use of the available N^{3}LO QCD predictions for hard scattering cross sections for key processes [5–8] in proton-proton collisions at the LHC as well as for structure functions in deep-inelastic electron-proton scattering (DIS) probed by the EIC [9–11].

The PDFs of quarks and antiquarks of flavour i and of the gluon, $q_i(x,\mu^2)$, $\bar{q}_i(x,\mu^2)$ and $g(x,\mu^2)$, are given by the respective number distributions in the fractional hadron momentum x at the factorization scale μ. For n_f flavours, the flavour-summed quark distributions

$$q_{\rm s}(x,\mu^2) = \sum_{i=1}^{n_f} \Big[q_i(x,\mu^2) + \bar{q}_i(x,\mu^2) \Big] \tag{1}$$

define the singlet quark distribution $q_{\rm s}$, which mixes under QCD evolution with the gluon distribution g through the matrix of splitting functions $P_{\rm ij}$ as

$$\frac{d}{d\ln\mu^2} \begin{pmatrix} q_{\rm s} \\ g \end{pmatrix} = \begin{pmatrix} P_{\rm qq} & P_{\rm qg} \\ P_{\rm gq} & P_{\rm gg} \end{pmatrix} \otimes \begin{pmatrix} q_{\rm s} \\ g \end{pmatrix} \tag{2}$$

where $\otimes$ stands for the Mellin convolution in the momentum variable x. The perturbative expansion in the strong coupling with $a_{\rm s} \equiv \alpha_{\rm s}(\mu^2)/(4\pi)$ can be written as

* Corresponding author.
E-mail address: sven-olaf.moch@desy.de (S. Moch).

https://doi.org/10.1016/j.physletb.2023.137944

$$P_{\rm ij}\,(x,\alpha_{\rm s}) = \sum_{n=0} a_{\rm s}^{n+1}\, P_{\rm ij}^{(n)}(x)\ , \tag{3}$$

such that the terms $P_{\rm ij}^{(k)}$ correspond to the QCD predictions at N^{k}LO accuracy. Here and below we identify, without loss of information, the renormalization scale with the scale μ in eq. (1).

The quark-quark splitting function $P_{\rm qq}$ in eq. (2) is the sum $P_{\rm qq} = P_{\rm ns}^{+} + P_{\rm ps}$, where $P_{\rm ns}^{+}$ denotes the splitting function for non-singlet combinations of the quark-antiquark sums $q_i + \bar{q}_i$, and $P_{\rm ps}$ is the pure-singlet contribution. The results for the four-loop (N^{3}LO) non-singlet splitting functions $P_{\rm ns}^{(3)}$ are complete in the planar limit, i.e., the large-n_c limit of a colour SU(n_c) gauge group, and very good approximations for the remaining non-planar terms have been obtained [12,13].

In this letter, we address the computation of the pure-singlet part $P_{\rm ps}^{(3)}$ at N^{3}LO. Together with the result for $P_{\rm ns}^{(3)+}$, this provides the quark-quark splitting functions at four loops. We present analytic results for the first 10 even Mellin moments $N \leq 20$ of $P_{\rm ps}^{(3)}(x)$, valid for a general compact simple gauge group. These correspond (up to a negative sign, which is a standard convention) to the anomalous dimensions $\gamma_{\rm ps}^{(3)}$,

$$\gamma_{\rm ij}^{(n)}(N) = -\int_0^1 dx\; x^{N-1}\, P_{\rm ij}^{(n)}(x)\ . \tag{4}$$

This extends previous results on this function, which is already known in the limit of large numbers of flavours n_f [14]. Following the approach of refs. [2,3] via physical quantities in inclusive DIS, also low moments ($N \leq 8$) of $P_{\rm ps}^{(3)}$ have been presented before [15], which have been used in approximations [16] for applications in N^{3}LO PDF fits. For the parts proportional to the quartic colour factor $d_R^{abcd} d_R^{abcd}$ (see below), the moments up to $N = 16$ have been derived [17] by computing anomalous dimensions of off-shell flavour-singlet operator matrix elements (OMEs).

Here we extend the method of OMEs further. The starting point is the standard set of the spin-N twist-two irreducible flavour-singlet quark and gluon operators, given by

$$\begin{aligned} O_{\rm q}^{\{\mu_1,\ldots,\mu_N\}} &= \frac{1}{2}\,\overline{\psi}\,\gamma^{\{\mu_1} D^{\mu_2} \ldots D^{\mu_N\}}\,\psi \;+\; \text{traceless}\,, \\ O_{\rm g}^{\{\mu_1,\ldots,\mu_N\}} &= \frac{1}{2}\,F^{\nu\{\mu_1} D^{\mu_2} \cdots D^{\mu_{N-1}}\, F^{\mu_N\}}_{\ \ \nu} \;+\; \text{traceless}\,, \end{aligned} \tag{5}$$

where ψ represents the quark field, $F_{\mu\nu}$ the gluon field-strength tensor and $D_\mu = \partial_\mu - {\rm i}gA_\mu$ the covariant derivative with the coupling g, where $g^2/(4\pi) = \alpha_{\rm s}$. The curly brackets $\{\ldots\}$ denote symmetrization. Flavour non-singlet operators have been discussed in ref. [12].

Contraction of the Lorentz indices with N identical light-like ($\Delta.\Delta = 0$) vectors Δ^μ allows for a compact notation in terms of the quantities

$$F^{\mu;a} = \Delta_\nu\, F^{\mu\nu;a}\,, \qquad A^a = \Delta_\mu\, A^{\mu;a}\,, \qquad D = \Delta_\mu\, D^\mu\,, \qquad \partial = \Delta_\mu\, \partial^\mu\,, \tag{6}$$

with labels a in the adjoint representation of the colour gauge group. The projection of eq. (5) defines the scalar operators for even N (suppressing the index N here and below) as

$$O_{\rm q} = \frac{1}{2}\,\overline{\psi}\not{\Delta} D^{N-2}\,\psi\,, \qquad O_{\rm g} = \frac{1}{2}\,F_\nu^{\ a}\, D_{ab}^{N-2}\, F^{\nu;b}\,. \tag{7}$$

These physical (gauge-invariant) operators, when evaluated in general Green's functions, mix under renormalization with non-physical, so-called alien operators, which also involve (anti-)ghost fields $\overline{c}$ and c. The general theory of the renormalization of gauge-invariant operators has been worked out in a series of classical papers by Dixon and Taylor [18], Kluberg-Stern and Zuber [19,20] and Joglekar and Lee [21–23]. These led the way to explicit computations at two loops in ref. [24], which solved an issue that had beset the pioneering calculation of ref. [25], and refs. [26,27]. Recently, the complete three-loop renormalization via a direct calculation of the alien counter-terms has been published [28].

A general procedure to construct the basis of alien operators was formulated by two of us in ref. [29] and was used to construct an explicit basis up to four loops for any fixed spin N. Building on this work, we here consider the four-loop renormalization of singlet quark operators. For this we need two sets of alien operators, $O_A^i = O_{\rm q}^i + O_{\rm g}^i + O_{\rm c}^i$ with $i = I, II$, which read

$$\begin{aligned} O_{\rm q}^I &= \eta\, g\, \overline{\psi}\not{\Delta}\, t^a\, \psi\, \left(\partial^{N-2} A_a\right)\,, \\ O_{\rm g}^I &= \eta\, (D.F)^a \left(\partial^{N-2} A_a\right)\,, \\ O_{\rm c}^I &= -\eta\, \left(\partial\, \overline{c}^a\right) \left(\partial^{N-1} c_a\right) \end{aligned} \tag{8}$$

with a coupling η which is a function of N and $\alpha_{\rm s}$, and

$$\begin{aligned} O_q^{II} &= g^2\, \overline{\psi}\not{\Delta}\, t_a\, \psi \sum_{i+j=N-3} \kappa_{ij}\, f^{abc} \left(\partial^i A_b\right) \left(\partial^j A_c\right)\,, \\ O_g^{II} &= g\, (D.F)_a \sum_{i+j=N-3} \kappa_{ij}\, f^{abc} \left(\partial^i A_b\right) \left(\partial^j A_c\right)\,, \\ O_c^{II} &= -g \sum_{i+j=N-3} \eta_{ij}\, f^{\,abc}\, \left(\partial\, \overline{c}_a\right) \left(\partial^{\,i} A_b\right) \left(\partial^{\,j+1} c\right)\,, \end{aligned} \tag{9}$$

where t^a (f^{abc}) denote the fundamental (adjoint) colour-group generators. The couplings η_{ij} and κ_{ij} obey constraints due to the (anti-) BRST symmetry of the alien operators [29], viz

$$\eta_{ij} = -\sum_{s=0}^{i}(-1)^{s+j}\binom{s+j}{s}\eta_{(i-s)(j+s)} = 2\kappa_{ij} + \eta\binom{i+j+1}{i}. \tag{10}$$

Hence the κ_{ij} are dependent on the η_{ij} for which we obtain a compact expression in terms of binomial coefficients

$$\eta_{ij} = \eta\left[(-1)^i - 3\binom{N-2}{i} - \binom{N-2}{i+1}\right], \tag{11}$$

where, in the present case, the coupling $\eta = \eta(\alpha_s, N)$ from eq. (8) is found to factorize to the loop-order required.

The physical operators in eq. (7) mix under renormalization with the alien ones in eqs. (8) and (9). The latter are summarized from now on collectively as O_A and we denote renormalized operators as $[O]_i$, so that

$$\begin{pmatrix} O_q \\ O_g \\ O_A \end{pmatrix} = \begin{pmatrix} Z_{qq} & Z_{qg} & Z_{qA} \\ Z_{gq} & Z_{gg} & Z_{gA} \\ Z_{Aq} & Z_{Ag} & Z_{AA} \end{pmatrix} \begin{pmatrix} [O]_q \\ [O]_g \\ [O]_A \end{pmatrix}, \tag{12}$$

where the Z-factors are determined in terms of the anomalous dimensions γ_{ij} in eq. (4) (and the corresponding ones γ_{qA}, γ_{gA} etc. including the alien operators) through the standard renormalization group equation

$$\mu^2\frac{d}{d\mu^2}Z_{ij} = \left(\beta(\alpha_s)\frac{\partial}{\partial\alpha_s} + \gamma_3\,\xi\,\frac{\partial}{\partial\xi}\right)Z_{ij} = -\gamma_{ik}\,Z_{kj}\,. \tag{13}$$

Here β is the QCD β-function and γ_3 the gluon anomalous dimension, all known to a more than sufficiently high order [30–33]. The Z_{ij} involving the alien operators can be gauge dependent, ξ is the gauge parameter with $\xi = 1$ for Feynman gauge. Moreover, since the alien operators cannot mix into the set of physical operators [21–23], the entries Z_{Aq} and Z_{Ag} in eq. (12) have to vanish.

The setup of our OME computations follows previous work [12,17]. The necessary Feynman rules are determined from eqs. (7)–(11), which are sufficient for the present computations. The diagrams for the OMEs $A_{ij} = \langle j(p)|\,O_i\,|j(p)\rangle$ with (physical or alien) spin-N twist-two operators O_i inserted in Green's functions with off-shell quarks, gluons or ghosts have been generated using QGRAF [34] and then processed, see ref. [35], by a FORM [36–38] program which collects self-energy insertions, determines the colour factors [39] and classifies the topologies according to the conventions of the FORCER package [40]. For computational efficiency, diagrams with the same colour factor and topology are merged into meta-diagrams.

An optimized in-house version of FORCER, briefly discussed in ref. [13], is employed to perform the integral reductions for fixed integer values of N. In practice, the range in N is limited by the occurrence of high powers of scalar products in the loop integrals for high values of N, which lead to large-size expressions and long computing times in the topology transformations and parametric reductions encoded in FORCER. The divergences in the OMEs A_{ij} are treated in dimensional regularization with $D = 4 - 2\epsilon$ dimensions, hence the Z-factors in eq. (12) are simple Laurent series in ϵ and the anomalous dimensions γ_{ij} can be read off from their single poles $1/\epsilon$.

For the quark-quark splitting functions, the physical OMEs A_{qq} have been obtained at even $N \leq 20$ up to four loops. This includes both the flavour non-singlet parts [13] and the pure-singlet contributions addressed in the present letter. The physical OMEs A_{qg}, A_{gq} and A_{gg} and those with the alien operators inserted into a quark two-point function, A_{Aq}, have been computed up to three loops. All others were needed at two loops only for the extraction of $P_{ps}^{(3)}$ at four loops using eq. (13). This leads to the following results for the N^{3}LO contributions to the pure-singlet anomalous dimensions in eq. (4) for QCD, i.e., the gauge group SU($n_c = 3$),

$$\begin{aligned}
\gamma_{ps}^{(3)}(N=2) &= -691.5937093\,n_f + 84.77398149\,n_f^2 + 4.466956849\,n_f^3\,,\\
\gamma_{ps}^{(3)}(N=4) &= -109.3302335\,n_f + 8.776885259\,n_f^2 + 0.306077137\,n_f^3\,,\\
\gamma_{ps}^{(3)}(N=6) &= -46.03061374\,n_f + 4.744075766\,n_f^2 + 0.042548957\,n_f^3\,,\\
\gamma_{ps}^{(3)}(N=8) &= -24.01455020\,n_f + 3.235193483\,n_f^2 - 0.007889256\,n_f^3\,,\\
\gamma_{ps}^{(3)}(N=10) &= -13.73039387\,n_f + 2.375018759\,n_f^2 - 0.021029241\,n_f^3\,,\\
\gamma_{ps}^{(3)}(N=12) &= -8.152592251\,n_f + 1.819958178\,n_f^2 - 0.024330231\,n_f^3\,,\\
\gamma_{ps}^{(3)}(N=14) &= -4.840447180\,n_f + 1.438327380\,n_f^2 - 0.024479943\,n_f^3\,,\\
\gamma_{ps}^{(3)}(N=16) &= -2.751136330\,n_f + 1.164299642\,n_f^2 - 0.023546009\,n_f^3\,,\\
\gamma_{ps}^{(3)}(N=18) &= -1.375969240\,n_f + 0.960873318\,n_f^2 - 0.022264393\,n_f^3\,,\\
\gamma_{ps}^{(3)}(N=20) &= -0.442681568\,n_f + 0.805745333\,n_f^2 - 0.020918264\,n_f^3\,.
\end{aligned} \tag{14}$$

The results for $N \leq 8$ agree with those obtained via cross sections for inclusive DIS in ref. [15]. As a further check, we have extended those DIS computations of $P_{ps}^{(3)}$ to $N = 10$ and $N = 12$, their results also agree with eq. (14). The large-n_f parts agree with all-N results of ref. [14]. In addition, the renormalization constants involving alien operators agree to the loop order required here with those recently published in ref. [28].

The analytic expressions for $\gamma_{ps}^{(3)}$ for a general gauge group are given in Appendix A in eqs. (A.3)–(A.12). They contain rational numbers and Riemann-ζ values, i.e. ζ_n with $n = 3, 4, 5$. New all-N results for $\gamma_{ps}^{(3)}$ based on eqs. (A.3)–(A.12) and, in cases, even higher fixed-N OME

computations, have been derived for specific colour factors or terms proportional to certain Riemann-ζ values. They can be expressed in terms harmonic sums [41,42], which are recursively defined by

$$S_{\pm m_1,m_2,\ldots,m_d}(N) \;=\; \sum_{i=1}^{N} \frac{(\pm 1)^i}{i^{m_1}}\, S_{m_2,\ldots,m_d}(i) \;, \tag{15}$$

and their weight w is the sum of the absolute values of the indices m_d. In the results for the n-loop anomalous dimensions, quantities up to $w = 2\,n-1$ occur, which can be composed of harmonic sums, Riemann-ζ_m values ($m \geq 3$), and simple denominators, $D_a^k = (N+a)^{-k}$. The latter count as objects of weight m and k, respectively. Due to (partial) conformal symmetry, especially the sums with the highest weights often arise with two specific (reciprocity respecting, cf. the discussion in ref. [12]) combinations of simple denominators,

$$\eta \equiv \frac{1}{N} - \frac{1}{N+1} \;\equiv\; D_0 - D_1 \;=\; \frac{1}{N(N+1)} \;, \tag{16}$$

$$\nu \equiv \frac{1}{N-1} - \frac{1}{N+2} \;\equiv\; D_{-1} - D_2 \;=\; \frac{3}{(N-1)(N+2)} \;. \tag{17}$$

With this notation (suppressing the argument N of the harmonic sums for brevity), we can summarize the known and new all-N results for $\gamma_{\rm ps}^{(3)}$. The leading large-n_f contribution has been published in eq. (3.10) of ref. [14],

$$\begin{aligned}
\gamma_{\rm ps}^{(3)}(N)\big|_{n_f^3} = 16/9\,C_F \Big\{ & 2/3\left(2S_{1,1,1} - 3\zeta_3\right)\left(9\,\eta + 6\,\eta^2 - 4\,\nu\right) + 4/3\,S_{1,1}\left(11\,D_0 - 13\,D_0^2\right. \\
& \left. +6\,D_0^3 - 17\,D_1 - 4\,D_1^2 + 12\,D_1^3 + 2\,D_2 + 8\,D_2^2 + 4\,D_{-1}\right) - 2/9\,S_1\left(94\,D_0 - 98\,D_0^2 + 87\,D_0^3\right. \\
& \left. -18\,D_0^4 - 226\,D_1 + 100\,D_1^2 + 111\,D_1^3 - 90\,D_1^4 + 128\,D_2 + 88\,D_2^2 - 48\,D_2^3 + 4\,D_{-1}\right) \\
& +1/9\left(52\,D_0 - 118\,D_0^2 + 146\,D_0^3 - 87\,D_0^4 + 18\,D_0^5 - 412\,D_1 + 430\,D_1^2 - 54\,D_1^3 - 309\,D_1^4\right. \\
& \left. +198\,D_1^5 + 364\,D_2 + 72\,D_2^2 - 176\,D_2^3 + 96\,D_2^4 - 4\,D_{-1}\right)\Big\} .
\end{aligned} \tag{18}$$

Additional all-N information can be obtained for the terms involving Riemann-ζ values, due to the reduced complexity of the harmonic sums. The reconstruction of the all-N expressions follows the same approach as in the nonsinglet case in ref. [12]. The ζ_3 dependence of the quartic colour factor $d_R^{abcd} d_R^{abcd}/n_c$ is given by (see Appendix A for the definition of all colour factors),

$$\begin{aligned}
\gamma_{\rm ps}^{(3)}(N)\Big|_{\zeta_3\, n_f\, d_R^{abcd} d_R^{abcd}/n_c} = 256\Big\{ & \left(S_3 + 4S_{-2,1} - 2S_{-3}\right)\left(3 - 6\eta\right) \\
& + \left(2S_{1,1} - S_2\right)\left(27\eta + 22\eta^2 - 32/3\nu\right) + S_{-2}\left(-1/3 + 92/3\eta + 20\eta^2 - 32/3\nu\right) \\
& + S_1\left(-70\eta - 68\eta^2 - 24\eta^3 + 64/3\nu\right) + 8/3\eta - 3\eta^2\Big\} .
\end{aligned} \tag{19}$$

This is a new result based on computing the relevant OMEs for $N \leq 22$. Likewise, for the colour factor $n_f^2\,C_F^2$ the term proportional to ζ_3 reads

$$\begin{aligned}
\gamma_{\rm ps}^{(3)}(N)\Big|_{\zeta_3\, n_f^2\, C_F^2} = 32/9\Big\{ & 2\,S_1\,(9\,\eta + 6\,\eta^2 - 4\,\nu) - 335\,D_0 + 145\,D_0^2 - 66\,D_0^3 \\
& + 287\,D_1 + 187\,D_1^2 + 90\,D_1^3 + 36\,D_2 + 8\,D_2^2 + 12\,D_{-1} - 16\,D_{-1}^2\Big\} ,
\end{aligned} \tag{20}$$

which is new as well. This expression has been derived from and verified using moments up to $N = 52$, which are part of the computations of the n_f^2 QED contributions to $\gamma_{\rm ij}^{(3)}$ to very high N [43].

Next, the ζ_4 part in $\gamma_{\rm ps}^{(3)}(N)$ can be derived with the help of the no-π^2 conjecture/theorem [44,45]. This has been done in ref. [46], eq. (9).[1] Eqs. (A.3)–(A.12) agree with this result,

$$\begin{aligned}
\gamma_{\rm ps}^{(3)}(N)\Big|_{\zeta_4} = 16\,C_F\,(C_A - C_F)\Big\{ & C_F\,n_f\left(46\,\nu - 8\,\nu^2 - 117\,\eta - 87\,\eta^2 - 18\,\eta^3\right) \\
& + (C_A - C_F)\,n_f\left(38\,\nu - 8\,\nu^2 - 195/2\,\eta - 69\,\eta^2 - 12\,\eta^3 + S_1\,(8\,\nu - 18\,\eta - 12\,\eta^2)\right) \\
& + n_f^2\left(15\,\eta + 10\,\eta^2 - 20/3\,\nu\right)\Big\} .
\end{aligned} \tag{21}$$

Finally, with the moments up to $N = 20$ the terms with ζ_5 can be readily determined and verified for all colour factors, thus extending the result in eq. (3.13) ref. [17], where the all-N ζ_5 contributions to the quartic colour factors have been given,

[1] The coefficients proportional to ν in eqs. (9) and (12) in ref. [46] need to be replaced as follows: $\nu \to \nu/3$. Note further that the definition of ν in ref. [14] differs from that in ref. [17] and the present paper by this factor of 3.

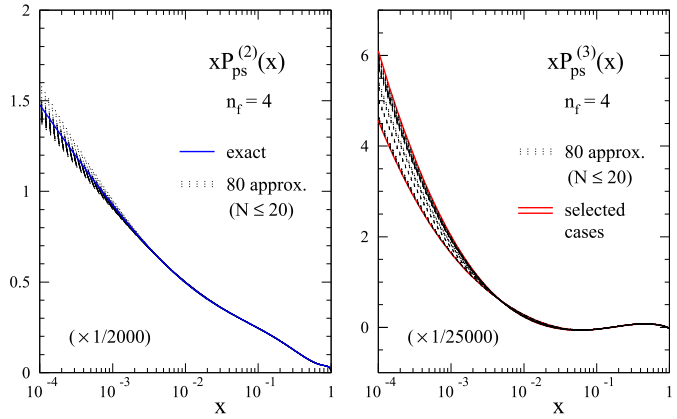

Fig. 1. 80 trial functions, constructed as described in the text, for the splitting functions $P_{\rm ps}^{(n)}(x)$ at $n_f = 4$. At $n = 2$ (left panel) the known exact result is shown by the solid (blue) line. At $n = 3$ (right panel) two functions, shown by the solid (red) lines, are chosen to represent the remaining uncertainty.

$$\begin{aligned}\gamma_{\rm ps}^{(3)}(N)\Big|_{\zeta_5} &= 160\,n_f\,C_F^3\left(9\,\eta + 6\,\eta^2 - 4\,\nu\right) + 80/3\,n_f\,C_A\,C_F^2\left(-9\,\eta - 6\,\eta^2 + 4\,\nu\right)\\ &+ 40/9\,n_f\,C_A^2\,C_F\left(-1 - 214\,\eta - 144\,\eta^2 + 104\,\nu\right)\\ &+ 320/3\,n_f\,\frac{d_R^{abcd}d_R^{abcd}}{n_c}\left(-1 + 56\,\eta + 36\,\eta^2 - 16\,\nu\right).\end{aligned} \tag{22}$$

Expressions in x-space for the leading large-n_f part of eq. (18) have been presented in ref. [14], eq. (4.21). On the other hand, the N-space terms with Riemann-ζ values do not correspond to the x-space contributions with Riemann-ζ values, as the inverse Mellin transformation generates additional terms with ζ_n. Similarly, it is not possible to read off the coefficients of ζ_n in the limit $N \to \infty$ from eqs. (19)–(22), as non-ζ harmonic sums contribute to these.

For phenomenology applications, the moments in eq. (14) can be used to construct approximate representations for the n_f^1 and n_f^2 parts of $P_{\rm ps}^{(3)}(x)$, subject to the constraints imposed by the known terms in the limits $x \to 0,\ 1$. At small x, the coefficient of the leading logarithm $(\ln^2 x)/x$ is known since long [47], as well as those of the highest three sub-dominant logarithms $\ln^k x$ with $k = 6, 5, 4$, see ref. [48]. At large x, the leading terms are of the form $(1-x)^j \ln^k(1-x)$ with $j \geq 1$ and $k \leq 4$. The coefficients for $k = 4, 3$ are known [49] for all j. With the 10 Mellin moments $N \leq 20$ in eq. (14), the coefficients of all remaining unknown small-x and large-x (for $j = 1$) terms can be 'fitted' together with a three-parameter interpolating function. Thus all approximations include

- the next-to-leading and next-to-next-to-leading small-x terms: $(\ln x)/x$ and $1/x$,
- the remaining three sub-dominant small-x logarithms: $\ln^k x$ with $k = 3, 2, 1$,
- the two remaining $j = 1$ large-x terms: $(1-x)\ln^k(1-x)$ with $k = 2, 1$.

Choosing 10 two-parameter polynomials together one function that includes $\ln^k(1-x)$ with $k = 1$ or 2 or the dilogarithm $\mathrm{Li}_2(x)$ (suitably suppressed as $x \to 1$), we have thus built 80 trial functions that fulfil all known constraints. These functions are shown $n_f = 4$ by the black-dotted curves in the right part of Fig. 1; other values of n_f show qualitatively the same behaviour. As a check, exactly the same procedure has been applied to the NNLO splitting function $P_{\rm ps}^{(2)}(x)$, where it can be compared with the exact result [3]; this comparison is shown in the left part of the figure.

Since our approximation procedure passes this test (and others), we have selected two representatives for each physically relevant value of n_f that indicate the remaining uncertainty in $P_{\rm ps}^{(3)}(x)$. The chosen approximation, shown in red in Fig. 1, are, with $x_1 = 1 - x$, $L_1 = \ln(1-x)$ and $L_0 = \ln x$,

$$\begin{aligned}P_{\rm ps,\,A}^{(3)}(n_f = 3, x) &= p_{\rm ps,0}^{(n_f=3)}(x) + 67731\,x_1 L_0/x + 274100\,x_1/x + 40006\,L_0^3 + 10620\,L_0^2\\ &+ 353656\,x_1 L_0 - 2365.1\,x_1 L_1^2 - 7412.1\,x_1 L_1 + 1533.0\,x_1^2 L_1^2 - 104493\,x_1(1+2x) + 34403\,x_1 x^2\,,\\ P_{\rm ps,\,B}^{(3)}(n_f = 3, x) &= p_{\rm ps,0}^{(n_f=3)}(x) + 54593\,x_1 L_0/x + 179748\,x_1/x - 2758.3\,L_0^3 - 103604\,L_0^2\\ &+ 4700.0\,x_1 L_0 - 1986.9\,x_1 L_1^2 - 2801.2\,x_1 L_1 - 6005.9\,x_1^2 L_1^2 - 195263\,x_1 + 12789\,x_1 x(1+x)\,,\end{aligned} \tag{23}$$

$$\begin{aligned}P_{\rm ps,\,A}^{(3)}(n_f = 4, x) &= p_{\rm ps,0}^{(n_f=4)}(x) + 90154\,x_1 L_0/x + 359084\,x_1/x + 52525\,L_0^3 + 13869\,L_0^2\\ &+ 461167\,x_1 L_0 - 2491.5\,x_1 L_1^2 - 7498.2\,x_1 L_1 + 1727.2\,x_1^2 L_1^2 - 136319\,x_1(1+2x) + 45379\,x_1 x^2\,,\\ P_{\rm ps,\,B}^{(3)}(n_f = 4, x) &= p_{\rm ps,0}^{(n_f=4)}(x) + 72987\,x_1 L_0/x + 235802\,x_1/x - 3350.9\,L_0^3 - 135378\,L_0^2\\ &+ 5212.9\,x_1 L_0 - 1997.2\,x_1 L_1^2 - 1472.7\,x_1 L_1 - 8123.3\,x_1^2 L_1^2 - 254921\,x_1 + 17138\,x_1 x(1+x)\,,\end{aligned} \tag{24}$$

$$\begin{aligned}P_{\rm ps,\,A}^{(3)}(n_f = 5, x) &= p_{\rm ps,0}^{(n_f=5)}(x) + 112481\,x_1 L_0/x + 440555\,x_1/x + 64577\,L_0^3 + 16882\,L_0^2\\ &+ 562992\,x_1 L_0 - 2365.7\,x_1 L_1^2 - 6570.1\,x_1 L_1 + 1761.7\,x_1^2 L_1^2 - 166581\,x_1(1+2x) + 56087\,x_1 x^2\,,\end{aligned}$$

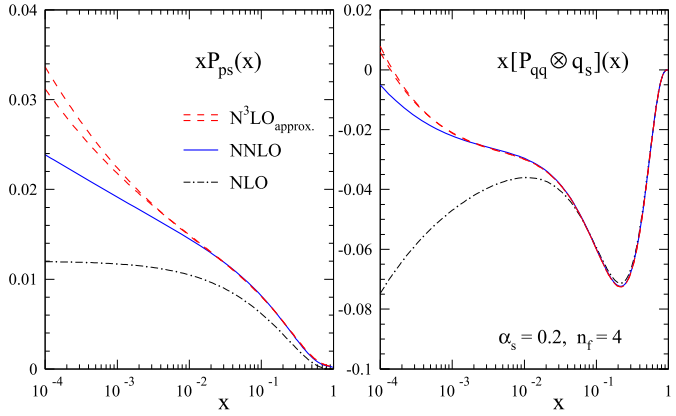

Fig. 2. Left: The NLO, NNLO and N^{3}LO approximations for $P_{\rm ps}(x)$ for a fixed value $\alpha_s(\mu_0^2) = 0.2$ of the strong coupling and $n_f = 4$. Right: The resulting perturbative expansion of the contribution of $P_{\rm qq}$ to the scale derivative of the singlet quark PDF q_s in eq. (2) for the initial distribution (28).

$$P^{(3)}_{\rm ps,\,B}(n_f = 5, x) = p^{(n_f=5)}_{\rm ps,0}(x) + 91468\,x_1 L_0/x + 289658\,x_1/x - 3814.9\,L_0^3 - 165795\,L_0^2 + 4908.9\,x_1 L_0 - 1760.8\,x_1 L_1^2 + 804.5\,x_1 L_1 - 10295\,x_1^2 L_1^2 - 311749\,x_1 + 21521\,x_1 x(1+x)\,, \tag{25}$$

with the known endpoint contribution, with coefficients rounded to seven significant figures,

$$p^{(n_f)}_{\rm ps,0}(x) = n_f \Big\{ 1749.227\,L_0^2/x - (7.506173 - 0.7901235\,n_f) L_0^6 + (28.54979 + 3.792593\,n_f) L_0^5 - (854.8001 - 77.36626\,n_f + 0.1975309\,n_f^2) L_0^4 - (199.1111 - 13.69547\,n_f) x_1^2 L_1^3 - 13.16872\,x_1^2 L_1^4 - (247.5505 - 40.55967\,n_f + 1.580247\,n_f^2) x_1 L_1^3 - (56.46091 - 3.621399\,n_f) x_1 L_1^4 \Big\}\,. \tag{26}$$

Specifically, we note that eqs. (23)–(25) include a numerical prediction, with a precision of ±10%, of the so far uncalculated coefficient of the next-to-leading small-x logarithm $(\ln x)/x$ of $P^{(3)}_{\rm ps}(x)$ for $n_f = 3, 4, 5$. The above uncertainty bands also lead to the following predictions for the $\gamma^{(3)}_{\rm ps}(N)$ at $N = 22$ (with brackets indicating the error on the last digits),

$$\gamma^{(3)}_{\rm ps}(N = 22) \;=\; 6.2478570(6)\,,\;\; 10.5202730(8)\,,\;\; 15.6913948(10) \quad \text{for} \quad n_f \;=\; 3, 4, 5\,. \tag{27}$$

The numerical implications for the evolution of q_s due to the quark-quark splitting functions in eq. (24) are illustrated in Fig. 2 for our default value $n_f = 4$. We show the perturbative expansion for $P_{\rm ps}$ alone and for the convolution $P_{\rm qq} \otimes q_s$ through N^{3}LO, in the latter case using the same schematic (order-independent) model input [3] for the singlet quark PDF in eq. (1),

$$x q_s(x, \mu_0^2) \;=\; 0.6\,x^{-0.3}(1-x)^{3.5}\left(1 + 5.0\,x^{0.8}\right)\,, \tag{28}$$

together with $\alpha_s(\mu_0^2) = 0.2$. The latter value of the strong coupling corresponds to scales in the range $\mu_0^2 \simeq 25 \ldots 50$ GeV^2 for $\alpha_s(M_Z^2) = 0.114 \ldots 0.120$ beyond the leading order. This fixed input facilitates a direct comparison of effects of the various perturbative order for the splitting function $P_{\rm qq} = P^+_{\rm ns} + P_{\rm ps}$, where the four-loop results for $P^{(3)+}_{\rm ns}$ have been taken from refs. [12,13].

Fig. 2 shows that the convolution of the splitting functions with q_s dampens the residual small-x uncertainties induced by the approximations A and B in eq. (24). The uncertainties in these convolutions are practically negligible down to $x \lesssim 10^{-3}$ and, even if our error band were to underestimate the uncertainty by, say, a factor of 2, perfectly tolerable even at x as small as $x \approx 10^{-4}$. Further phenomenological studies, such as the scale stability of the parton evolution in eq. (2) under the variation of the renormalization scales require additional information at four loops on the other splitting functions $P_{\rm qg}$, $P_{\rm gq}$ and $P_{\rm gg}$. These will be subject of forthcoming publications.

With the four-loop results for the pure-singlet quark splitting function $P_{\rm ps}$ presented here, we have provided a major step towards improving the accuracy of the flavour-singlet parton evolution by one perturbative order beyond the current state of the art. The evolution of PDFs at N^{3}LO is expected to achieve percent-level precision, and a brief phenomenological study of our results is consistent with this expectation. We have shown that the knowledge of 10 Mellin moments of $P^{(3)}_{\rm ps}(x)$, together with the present knowledge of the behaviour at the endpoints $x \to 1$ and $x \to 0$, is sufficient for the construction of approximations that display negligible residual uncertainties in a wide kinematic range of parton momentum fractions x probed at current and future colliders.

Declaration of competing interest

The authors declare that they have no known competing financial interests or personal relationships that could have appeared to influence the work reported in this paper.

Data availability

No data was used for the research described in the article.

Acknowledgements

This work has been supported by the Vidi grant 680-47-551 of the Dutch Research Council (NWO), the UKRI FLF Mr/S03479x/1; the Consolidated Grant ST/P0000630/1 *Particle Physics at the Higgs Centre* of the UK Science and Technology Facilities Council (STFC); the ERC Starting Grant 715049 *QCDforfuture*; the Deutsche Forschungsgemeinschaft through the Research Unit FOR 2926, *Next Generation pQCD for Hadron Structure: Preparing for the EIC*, project number 40824754, and DFG grant MO 1801/4-2; and the STFC Consolidated Grant ST/T000988/1.

Appendix A. Mellin moments of $P_{\rm ps}^{(3)}$

Here we provide the exact results for the four-loop pure-singlet anomalous dimensions $\gamma_{\rm ps}^{(3)}(N)$ at even $N \le 20$ for a general compact simple gauge group. The numerical values in QCD, i.e., SU($n_c = 3$) have been given in eq. (14). The colour factors are $C_A = n_c$ and $C_F = (n_c^2 - 1)/(2n_c)$ for the quadratic Casimir invariants in SU(n_c). The relevant quartic colour factor $d_R^{abcd} d_R^{abcd}/n_c$ is obtained from the symmetrized trace of four generators T_r^a, see, e.g., [12,17,31],

$$d_r^{abcd} \;=\; \frac{1}{6}\,\mathrm{Tr}\,(\,T_r^a\,T_r^b\,T_r^c\,T_r^d \;+\; \text{five } bcd \text{ permutations}\,)\,, \tag{A.1}$$

with

$$\frac{d_R^{abcd} d_R^{abcd}}{n_c} \;=\; \frac{1}{96\,n_c^3}\,(n_c^2-1)(n_c^4-6\,n_c^2+18) \tag{A.2}$$

for the fundamental representation. In QCD: $C_A = 3$, $C_F = 4/3$ and $d_R^{abcd} d_R^{abcd}/n_c = 5/36$.

$$\begin{aligned}
\gamma_{\rm ps}^{(3)}(N=2) = {}& n_f\,C_F^3\left(\frac{227938}{2187}+\frac{1952}{81}\,\zeta_3+\frac{256}{9}\,\zeta_4-\frac{640}{3}\,\zeta_5\right)\\
&+ n_f\,C_A C_F^2\left(-\frac{162658}{6561}+\frac{8048}{27}\,\zeta_3-\frac{1664}{9}\,\zeta_4+\frac{320}{9}\,\zeta_5\right)\\
&+ n_f\,C_A^2\,C_F\left(-\frac{410299}{6561}-\frac{26896}{81}\,\zeta_3+\frac{1408}{9}\,\zeta_4+\frac{4480}{27}\,\zeta_5\right)\\
&+ n_f\,\frac{d_R^{abcd}d_R^{abcd}}{n_c}\left(\frac{1024}{9}+\frac{256}{9}\,\zeta_3-\frac{2560}{9}\,\zeta_5\right)+n_f^2\,C_F^2\left(-\frac{73772}{6561}-\frac{5248}{81}\,\zeta_3+\frac{320}{9}\,\zeta_4\right)\\
&+ n_f^2\,C_A C_F\left(\frac{160648}{6561}+48\,\zeta_3-\frac{320}{9}\,\zeta_4\right)+n_f^3\,C_F\left(-\frac{1712}{729}+\frac{128}{27}\,\zeta_3\right)\,,
\end{aligned} \tag{A.3}$$

$$\begin{aligned}
\gamma_{\rm ps}^{(3)}(N=4) = {}& n_f\,C_F^3\left(\frac{1995890620891}{52488000000}-\frac{897403}{202500}\,\zeta_3+\frac{18997}{2250}\,\zeta_4-\frac{484}{15}\,\zeta_5\right)\\
&+ n_f\,C_A\,C_F^2\left(\frac{209865827521}{26244000000}+\frac{6743539}{202500}\,\zeta_3-\frac{29161}{750}\,\zeta_4+\frac{242}{45}\,\zeta_5\right)\\
&+ n_f\,C_A^2\,C_F\left(-\frac{55187654921}{3280500000}-\frac{3104267}{67500}\,\zeta_3+\frac{34243}{1125}\,\zeta_4+\frac{3164}{135}\,\zeta_5\right)\\
&+ n_f\,\frac{d_R^{abcd}d_R^{abcd}}{n_c}\left(\frac{172231}{675}-\frac{5368}{25}\,\zeta_3-\frac{3728}{45}\,\zeta_5\right)+n_f^2\,C_F^2\left(-\frac{141522185707}{26244000000}-\frac{1207}{135}\,\zeta_3+\frac{242}{45}\,\zeta_4\right)\\
&+ n_f^2\,C_A\,C_F\left(\frac{9398360351}{1640250000}+\frac{57877}{10125}\,\zeta_3-\frac{242}{45}\,\zeta_4\right)+n_f^3\,C_F\left(-\frac{46099151}{72900000}+\frac{484}{675}\,\zeta_3\right)\,,
\end{aligned} \tag{A.4}$$

$$\begin{aligned}
\gamma_{\rm ps}^{(3)}(N=6) = {}& n_f\,C_F^3\left(\frac{140565274663259489}{5403265623000000}-\frac{62727544}{24310125}\,\zeta_3+\frac{343156}{77175}\,\zeta_4-\frac{1936}{147}\,\zeta_5\right)\\
&+ n_f\,C_A\,C_F^2\left(\frac{336481838777617}{360217708200000}+\frac{2111992}{324135}\,\zeta_3-\frac{1389806}{77175}\,\zeta_4+\frac{968}{441}\,\zeta_5\right)\\
&+ n_f\,C_A^2\,C_F\left(-\frac{6194882229735067}{864522499680000}-\frac{2396237}{165375}\,\zeta_3+\frac{41866}{3087}\,\zeta_4+\frac{9544}{1323}\,\zeta_5\right)\\
&+ n_f\,\frac{d_R^{abcd}d_R^{abcd}}{n_c}\left(\frac{64697569}{330750}-\frac{426976}{3675}\,\zeta_3-\frac{39808}{441}\,\zeta_5\right)\\
&+ n_f^2\,C_F^2\left(-\frac{812984663253277}{270163281150000}-\frac{2594876}{694575}\,\zeta_3+\frac{968}{441}\,\zeta_4\right)\\
&+ n_f^2\,C_A\,C_F\left(\frac{3092531515013}{964868861250}+\frac{217432}{99225}\,\zeta_3-\frac{968}{441}\,\zeta_4\right)+n_f^3\,C_F\left(-\frac{19597073837}{61261515000}+\frac{1936}{6615}\,\zeta_3\right)\,,
\end{aligned} \tag{A.5}$$

$$\gamma_{\rm ps}^{(3)}(N=8) = n_f\,C_F^3\left(\frac{3960340604223955458923}{192072198786048000000} - \frac{34718701049}{18003384000}\zeta_3 + \frac{13529827}{4762800}\zeta_4 - \frac{1369}{189}\zeta_5\right)$$
$$+ n_f\,C_A\,C_F^2\left(-\frac{43838488788848637899}{13719442770432000000} + \frac{10167760657}{18003384000}\zeta_3 - \frac{10211371}{952560}\zeta_4 + \frac{1369}{1134}\zeta_5\right)$$
$$+ n_f\,C_A^2\,C_F\left(-\frac{8552512702477166383}{2939880593664000000} - \frac{97528710971}{18003384000}\zeta_3 + \frac{1340251}{170100}\zeta_4 + \frac{128}{63}\zeta_5\right)$$
$$+ n_f\,\frac{d_R^{abcd}d_R^{abcd}}{n_c}\left(\frac{1183211180737}{7715736000} - \frac{18321694}{297675}\zeta_3 - \frac{18164}{189}\zeta_5\right)$$
$$+ n_f^2\,C_F^2\left(-\frac{5115927245667479753}{2743888554086400000} - \frac{15129691}{7144200}\zeta_3 + \frac{1369}{1134}\zeta_4\right)$$
$$+ n_f^2\,C_A\,C_F\left(\frac{15301312238130101}{7349701484160000} + \frac{8397097}{7144200}\zeta_3 - \frac{1369}{1134}\zeta_4\right)$$
$$+ n_f^3\,C_F\left(-\frac{162840799744061}{816633498240000} + \frac{1369}{8505}\zeta_3\right), \tag{A.6}$$

$$\gamma_{\rm ps}^{(3)}(N=10) = n_f\,C_F^3\left(\frac{1920665741173387739064931 3}{1118944450162341495000000} - \frac{45224548192}{28017383625}\zeta_3 + \frac{1080128}{539055}\zeta_4 - \frac{25088}{5445}\zeta_5\right)$$
$$+ n_f\,C_A\,C_F^2\left(-\frac{1538138456874500390560463}{298385186709957732000000} - \frac{31074715888}{28017383625}\zeta_3 - \frac{97295744}{13476375}\zeta_4 + \frac{12544}{16335}\zeta_5\right)$$
$$+ n_f\,C_A^2\,C_F\left(-\frac{2021791133045316447624 17}{284176368295197840000000} - \frac{192321673117627}{109828143810000}\zeta_3 + \frac{23430848}{4492125}\zeta_4 - \frac{14912}{49005}\zeta_5\right)$$
$$+ n_f\,\frac{d_R^{abcd}d_R^{abcd}}{n_c}\left(\frac{1240606813603}{9901861200} - \frac{182828576543}{6303268125}\zeta_3 - \frac{1624576}{16335}\zeta_5\right)$$
$$+ n_f^2\,C_F^2\left(-\frac{367710354086746558213}{296017050307497750000} + \frac{12544}{16335}\zeta_4 - \frac{1243744}{898425}\zeta_3\right)$$
$$+ n_f^2\,C_A\,C_F\left(\frac{314242565140920849001}{215285127496362000000} - \frac{12544}{16335}\zeta_4 + \frac{89550464}{121287375}\zeta_3\right)$$
$$+ n_f^3\,C_F\left(-\frac{2205751150439}{15885856515375} + \frac{25088}{245025}\zeta_3\right), \tag{A.7}$$

$$\gamma_{\rm ps}^{(3)}(N=12) = n_f\,C_F^3\left(\frac{8896171682921943271574032 1165467}{606570690962036286921314880 0000} - \frac{671898176890091}{475272972023850}\zeta_3\right.$$
$$\left. + \frac{2642589184}{1758511755}\zeta_4 - \frac{124820}{39039}\zeta_5\right)$$
$$+ n_f\,C_A\,C_F^2\left(-\frac{1166210765232575147065 41796876157}{194102621107851611814820761600 00} - \frac{1989733300788683}{1267394592063600}\zeta_3\right.$$
$$\left. - \frac{18419693641}{3517023510}\zeta_4 + \frac{62410}{117117}\zeta_5\right)$$
$$+ n_f\,C_A^2\,C_F\left(\frac{1085422424350545421242900455 99}{210067771761744168630758400000} + \frac{7458806358343849}{2281310265714480 00}\zeta_3\right.$$
$$\left. + \frac{108549713}{29066310}\zeta_4 - \frac{549260}{351351}\zeta_5\right)$$
$$+ n_f\,\frac{d_R^{abcd}d_R^{abcd}}{n_c}\left(\frac{1378902491887553593 9}{130167745507800000} - \frac{261789233833}{33202669500}\zeta_3 - \frac{11883280}{117117}\zeta_5\right)$$
$$+ n_f^2\,C_F^2\left(-\frac{2797424774494087428631891051}{3209368735248869242969920000} - \frac{15566147588}{15826605795}\zeta_3 + \frac{62410}{117117}\zeta_4\right)$$
$$+ n_f^2\,C_A\,C_F\left(\frac{1740051956313267953565 8867}{1615905936628801297159 6800} + \frac{536686847}{1055107053}\zeta_3 - \frac{62410}{117117}\zeta_4\right)$$
$$+ n_f^3\,C_F\left(-\frac{127821768039445576087}{1233139451029305019200} + \frac{24964}{351351}\zeta_3\right), \tag{A.8}$$

$$\gamma_{\rm ps}^{(3)}(N=14) = n_f\,C_F^3\left(\frac{3787159641416378852738541727085 51}{2969227158555422383530912000 0000} - \frac{367639947406454}{290813881483125}\zeta_3\right.$$
$$\left. + \frac{505959889}{430404975}\zeta_4 - \frac{22472}{9555}\zeta_5\right)$$

$$
\begin{aligned}
&+ n_f\, C_A\, C_F^2 \left(-\frac{15839103821892683237090057169 7207}{25124229803161266322184640000000} - \frac{14044584522181}{8616707599500}\zeta_3 \right.\\
&\left. - \frac{17190217637}{4304049750}\zeta_4 + \frac{11236}{28665}\zeta_5 \right)\\
&+ n_f C_A^2\, C_F \left(\frac{21261879383204556473931183 2977}{17178960549170096630553600000 0} + \frac{77579129461513987}{76774864711545000}\zeta_3 \right.\\
&\left. + \frac{933124519}{331080750}\zeta_4 - \frac{15356}{6615}\zeta_5 \right)\\
&+ n_f\, \frac{d_R^{abcd} d_R^{abcd}}{n_c} \left(\frac{19073114986773056430079}{207292134721171500000} + \frac{1655601644872528}{246073284331875}\zeta_3 - \frac{2945344}{28665}\zeta_5 \right)\\
&+ n_f^2\, C_F^2 \left(-\frac{40320685810576108505909420 23}{63445024755457743237840000 00} - \frac{14300095639}{19368223875}\zeta_3 + \frac{11236}{28665}\zeta_4 \right)\\
&+ n_f^2\, C_A\, C_F \left(\frac{15677247599879616342540623}{19014492933703619352000000} + \frac{72862649}{195638625}\zeta_3 - \frac{11236}{28665}\zeta_4 \right)\\
&+ n_f^3\, C_F \left(-\frac{1225131890207918292167}{15090867407701285200000} + \frac{22472}{429975}\zeta_3 \right) , \qquad \text{(A.9)}
\end{aligned}
$$

$$
\begin{aligned}
\gamma_{\rm ps}^{(3)}(N=16) = {}& n_f\, C_F^3 \left(\frac{52845922593469053066814397892836049514811}{47006470140548015345936823868698124800000} - \frac{1576051471675106357}{1378077594461568000}\zeta_3 \right.\\
&\left. + \frac{1209091491169}{1274723049600}\zeta_4 - \frac{18769}{10404}\zeta_5 \right)\\
&+ n_f\, C_A\, C_F^2 \left(-\frac{27213131661872043718027475800336596400 6181}{43089264295502347400442088546566144000000} - \frac{186362119838618569}{120140097978700800}\zeta_3 \right.\\
&\left. - \frac{805069021181}{254944609920}\zeta_4 + \frac{18769}{62424}\zeta_5 \right)\\
&+ n_f\, C_A^2\, C_F \left(\frac{10817813316292494855573317312252819634 6341}{64633896443253521100663132819849216000000} + \frac{12453233313645527413979}{7816915474984167552000}\zeta_3 \right.\\
&\left. + \frac{19557316769}{8852243400}\zeta_4 - \frac{131747}{46818}\zeta_5 \right)\\
&+ n_f\, \frac{d_R^{abcd} d_R^{abcd}}{n_c} \left(\frac{19475402774630131766348690 3}{23856468681439570176000000} + \frac{488331702547711013}{28175156700490800}\zeta_3 - \frac{808523}{7803}\zeta_5 \right)\\
&+ n_f^2\, C_F^2 \left(-\frac{27940032477586559318231174397709681}{58566283098537309493828740710400000} - \frac{220452248921}{382416914880}\zeta_3 + \frac{18769}{62424}\zeta_4 \right)\\
&+ n_f^2\, C_A\, C_F \left(\frac{51397902808930553670448344140631 91}{79129077348207578084492875776000 00} + \frac{1631966041}{5730523200}\zeta_3 - \frac{18769}{62424}\zeta_4 \right)\\
&+ n_f^3\, C_F \left(-\frac{13608819731912112034987483}{20666673809382141540679680 0} + \frac{18769}{468180}\zeta_3 \right) , \qquad \text{(A.10)}
\end{aligned}
$$

$$
\begin{aligned}
\gamma_{\rm ps}^{(3)}(N=18) = {}& n_f C_F^3 \left(\frac{72533595718924979539905767419648287312606227 09}{72411113066607126993803829278325441707520000 0} \right.\\
&\left. - \frac{109721806416706447798}{105229951281929298825}\zeta_3 + \frac{9447656272424}{12054216999825}\zeta_4 - \frac{236672}{165699}\zeta_5 \right)\\
&+ n_f\, C_A\, C_F^2 \left(-\frac{28959853818114889791771647893787915791563566723}{46854249631334023348931889533034109340160000 00} \right.\\
&\left. - \frac{751673700996836590582}{526149756409646494125}\zeta_3 - \frac{30932168351824}{12054216999825}\zeta_4 + \frac{118336}{497097}\zeta_5 \right)\\
&+ n_f\, C_A^2\, C_F \left(\frac{89162440521267641872038820315362221737605493}{45935538854249042498952832875523636608000000} \right.\\
&\left. + \frac{13230069684569021309898575 9}{67414515989255185999248000}\zeta_3 + \frac{50551793128}{28362863529}\zeta_4 - \frac{522368}{165699}\zeta_5 \right)\\
&+ n_f\, \frac{d_R^{abcd} d_R^{abcd}}{n_c} \left(\frac{26965803322442339116092009 2267}{36601787074498660542528000 00} + \frac{231728400575045385953}{9154108411989460920}\zeta_3 \right.\\
&\left. - \frac{17270272}{165699}\zeta_5 \right)
\end{aligned}
$$

$$+ n_f^2 C_F^2 \left(-\frac{5103205889313935590684511183228482172 63}{139307863658169281162087583645622560000} - \frac{10059181640656}{21697590599685}\zeta_3 + \frac{118336}{497097}\zeta_4 \right)$$
$$+ n_f^2 C_A C_F \left(\frac{57463607715346858669901353939920593 27}{109783849772832532297732967691456000 00} + \frac{24382094512}{108379573425}\zeta_3 - \frac{118336}{497097}\zeta_4 \right)$$
$$+ n_f^3 C_F \left(-\frac{12093315480521279173973861137}{22047074772836042891229067800 0} + \frac{236672}{7456455}\zeta_3 \right) , \tag{A.11}$$

$$\gamma_{\rm ps}^{(3)}(N=20) = n_f C_F^3 \left(\frac{21280324877276891233968911030814230028799458940 61}{23629885895942960079601673411279892336230400000 0} \right.$$
$$\left. - \frac{74630323856600125416449}{78044642230422968100 00}\zeta_3 + \frac{9834028074797}{14900178793500}\zeta_4 - \frac{178084}{153615}\zeta_5 \right)$$
$$+ n_f C_A C_F^2 \left(-\frac{84422817313490308915002823158837575 15259615913}{14132706875563971339474685054593237 04320000000} \right.$$
$$\left. - \frac{13512345939414493006 4021}{10405952297389729080000}\zeta_3 - \frac{7936779238702}{3725044698375}\zeta_4 + \frac{89042}{460845}\zeta_5 \right)$$
$$+ n_f C_A^2 C_F \left(\frac{25045010901821555366933375186326380712 3028219}{11901226842580186391136576888078515404 8000000} \right.$$
$$\left. + \frac{40625424437896114995230699}{18397723661785041013440000}\zeta_3 + \frac{164760066767}{112031419500}\zeta_4 - \frac{4694036}{1382535}\zeta_5 \right)$$
$$+ n_f \frac{d_R^{abcd} d_R^{abcd}}{n_c} \left(\frac{12404698801662978180931849946974 6921}{18401182433833456601150526720 00000} + \frac{34660205433264885994007}{11003423242694402520 00}\zeta_3 \right.$$
$$\left. - \frac{48237328}{460845}\zeta_5 \right)$$
$$+ n_f^2 C_F^2 \left(-\frac{20553091730130297702276618606953655791}{71772053747957053386934630643251200000} - \frac{2842660003013}{7450089396750}\zeta_3 + \frac{89042}{460845}\zeta_4 \right)$$
$$+ n_f^2 C_A C_F \left(\frac{68856002023137864639692721505113083 2957}{16027293205370860793924500226350080 00000} + \frac{1316792611}{7223745375}\zeta_3 - \frac{89042}{460845}\zeta_4 \right)$$
$$+ n_f^3 C_F \left(-\frac{46235817346069201871585241841}{99099338504205123418894560000 0} + \frac{178084}{6912675}\zeta_3 \right) . \tag{A.12}$$

The results for $\gamma_{\rm ps}^{(3)}$ at $N \leq 8$ in eqs. (A.3)–(A.6) have been published before in ref. [15], and the values at $N \leq 16$ of the terms proportional to the quartic group invariant $d_R^{abcd} d_R^{abcd}/n_c$ in eqs. (A.3)–(A.10) have already been obtained in ref. [17]. The n_f^3 contributions are known at all N [11].

A FORM file with our results for $\gamma_{\rm ps}(N)$ at even $N \leq 20$ and all partial all-N expressions in the main text, and a FORTRAN subroutine of our approximations for the splitting function $P_{\rm ps}^{(3)}(x)$ can be obtained from the preprint server `http://arXiv.org` by downloading the source. Furthermore they are available from the authors upon request.

References

[1] A. Accardi, et al., A critical appraisal and evaluation of modern PDFs, Eur. Phys. J. C 76 (2016) 471, arXiv:1603.08906.
[2] S. Moch, J.A.M. Vermaseren, A. Vogt, The three loop splitting functions in QCD: the non-singlet case, Nucl. Phys. B 688 (2004) 101–134, arXiv:hep-ph/0403192.
[3] A. Vogt, S. Moch, J.A.M. Vermaseren, The three-loop splitting functions in QCD: the singlet case, Nucl. Phys. B 691 (2004) 129–181, arXiv:hep-ph/0404111.
[4] R. Abdul Khalek, et al., Science requirements and detector concepts for the electron-ion collider: EIC yellow report, Nucl. Phys. A 1026 (2022) 122447, arXiv:2103.05419.
[5] C. Anastasiou, C. Duhr, F. Dulat, F. Herzog, B. Mistlberger, Higgs boson gluon-fusion production in QCD at three loops, Phys. Rev. Lett. 114 (2015) 212001, arXiv:1503.06056.
[6] C. Duhr, F. Dulat, B. Mistlberger, Drell-Yan cross section to third order in the strong coupling constant, Phys. Rev. Lett. 125 (2020) 172001, arXiv:2001.07717.
[7] X. Chen, T. Gehrmann, E.W.N. Glover, A. Huss, B. Mistlberger, A. Pelloni, Fully differential higgs boson production to third order in QCD, Phys. Rev. Lett. 127 (2021) 072002, arXiv:2102.07607.
[8] J. Baglio, C. Duhr, B. Mistlberger, R. Szafron, Inclusive production cross sections at N^{3}LO, J. High Energy Phys. 12 (2022) 066, arXiv:2209.06138.
[9] J.A.M. Vermaseren, A. Vogt, S. Moch, The third-order QCD corrections to deep-inelastic scattering by photon exchange, Nucl. Phys. B 724 (2005) 3–182, arXiv:hep-ph/0504242.
[10] S. Moch, J.A.M. Vermaseren, A. Vogt, Third-order QCD corrections to the charged-current structure function F_3, Nucl. Phys. B 813 (2009) 220–258, arXiv:0812.4168.
[11] J. Davies, A. Vogt, S. Moch, J.A.M. Vermaseren, Non-singlet coefficient functions for charged-current deep-inelastic scattering to the third order in QCD, PoS DIS2016 (2016) 059, arXiv:1606.08907.
[12] S. Moch, B. Ruijl, T. Ueda, J.A.M. Vermaseren, A. Vogt, Four-loop non-singlet splitting functions in the planar limit and beyond, J. High Energy Phys. 10 (2017) 041, arXiv:1707.08315.
[13] S. Moch, J.A.M. Vermaseren, A. Vogt, in press.
[14] J. Davies, A. Vogt, B. Ruijl, T. Ueda, J.A.M. Vermaseren, Large-n_f contributions to the four-loop splitting functions in QCD, Nucl. Phys. B 915 (2017) 335–362, arXiv:1610.07477.
[15] S. Moch, B. Ruijl, T. Ueda, J.A.M. Vermaseren, A. Vogt, Low moments of the four-loop splitting functions in QCD, Phys. Lett. B 825 (2022) 136853, arXiv:2111.15561.
[16] J. McGowan, T. Cridge, L.A. Harland-Lang, R.S. Thorne, Approximate N^{3}LO parton distribution functions with theoretical uncertainties: MSHT20aN^{3}LO PDFs, arXiv:2207.04739.
[17] S. Moch, B. Ruijl, T. Ueda, J.A.M. Vermaseren, A. Vogt, On quartic colour factors in splitting functions and the gluon cusp anomalous dimension, Phys. Lett. B 782 (2018) 627–632, arXiv:1805.09638.

[18] J.A. Dixon, J.C. Taylor, Renormalization of Wilson operators in gauge theories, Nucl. Phys. B 78 (1974) 552–560.
[19] H. Kluberg-Stern, J.B. Zuber, Renormalization of nonabelian gauge theories in a background field gauge. 1. Green functions, Phys. Rev. D 12 (1975) 482–488.
[20] H. Kluberg-Stern, J.B. Zuber, Renormalization of nonabelian gauge theories in a background field gauge. 2. Gauge invariant operators, Phys. Rev. D 12 (1975) 3159–3180.
[21] S.D. Joglekar, B.W. Lee, General theory of renormalization of gauge invariant operators, Ann. Phys. 97 (1976) 160.
[22] S.D. Joglekar, Local operator products in gauge theories. 1, Ann. Phys. 108 (1977) 233.
[23] S.D. Joglekar, Local operator products in gauge theories. 2, Ann. Phys. 109 (1977) 210.
[24] R. Hamberg, W.L. van Neerven, The correct renormalization of the gluon operator in a covariant gauge, Nucl. Phys. B 379 (1992) 143–171.
[25] E.G. Floratos, D.A. Ross, C.T. Sachrajda, Higher order effects in asymptotically free gauge theories. 2. Flavor singlet Wilson operators and coefficient functions, Nucl. Phys. B 152 (1979) 493–520.
[26] Y. Matiounine, J. Smith, W.L. van Neerven, Two loop operator matrix elements calculated up to finite terms, Phys. Rev. D 57 (1998) 6701–6722, arXiv:hep-ph/9801224.
[27] J. Blümlein, P. Marquard, C. Schneider, K. Schönwald, The two-loop massless off-shell QCD operator matrix elements to finite terms, Nucl. Phys. B 980 (2022) 115794, arXiv:2202.03216.
[28] T. Gehrmann, A. von Manteuffel, T.-Z. Yang, Renormalization of twist-two operators in covariant gauge to three loops in QCD, arXiv:2302.00022.
[29] G. Falcioni, F. Herzog, Renormalization of gluonic leading-twist operators in covariant gauges, J. High Energy Phys. 05 (2022) 177, arXiv:2203.11181.
[30] P.A. Baikov, K.G. Chetyrkin, J.H. Kühn, Five-loop running of the QCD coupling constant, Phys. Rev. Lett. 118 (2017) 082002, arXiv:1606.08659.
[31] F. Herzog, B. Ruijl, T. Ueda, J.A.M. Vermaseren, A. Vogt, The five-loop beta function of Yang-Mills theory with fermions, J. High Energy Phys. 02 (2017) 090, arXiv:1701.01404.
[32] T. Luthe, A. Maier, P. Marquard, Y. Schroder, The five-loop Beta function for a general gauge group and anomalous dimensions beyond Feynman gauge, J. High Energy Phys. 10 (2017) 166, arXiv:1709.07718.
[33] K.G. Chetyrkin, G. Falcioni, F. Herzog, J.A.M. Vermaseren, Five-loop renormalisation of QCD in covariant gauges, J. High Energy Phys. 10 (2017) 179, arXiv:1709.08541.
[34] P. Nogueira, Automatic Feynman graph generation, J. Comput. Phys. 105 (1993) 279–289.
[35] F. Herzog, B. Ruijl, T. Ueda, J.A.M. Vermaseren, A. Vogt, FORM, diagrams and topologies, PoS LL2016 (2016) 073, arXiv:1608.01834.
[36] J.A.M. Vermaseren, New features of FORM, arXiv:math-ph/0010025.
[37] J. Kuipers, T. Ueda, J.A.M. Vermaseren, J. Vollinga, FORM version 4.0, Comput. Phys. Commun. 184 (2013) 1453–1467, arXiv:1203.6543.
[38] B. Ruijl, T. Ueda, J. Vermaseren, FORM version 4.2, arXiv:1707.06453.
[39] T. van Ritbergen, A.N. Schellekens, J.A.M. Vermaseren, Group theory factors for Feynman diagrams, Int. J. Mod. Phys. A 14 (1999) 41–96, arXiv:hep-ph/9802376.
[40] B. Ruijl, T. Ueda, J.A.M. Vermaseren, Forcer, a FORM program for the parametric reduction of four-loop massless propagator diagrams, Comput. Phys. Commun. 253 (2020) 107198, arXiv:1704.06650.
[41] J.A.M. Vermaseren, Harmonic sums, Mellin transforms and integrals, Int. J. Mod. Phys. A 14 (1999) 2037–2076, arXiv:hep-ph/9806280.
[42] J. Blümlein, S. Kurth, Harmonic sums and Mellin transforms up to two loop order, Phys. Rev. D 60 (1999) 014018, arXiv:hep-ph/9810241.
[43] S. Moch, J. Vermaseren, A. Vogt, unpublished.
[44] M. Jamin, R. Miravitllas, Absence of even-integer ζ-function values in Euclidean physical quantities in QCD, Phys. Lett. B 779 (2018) 452–455, arXiv:1711.00787.
[45] P.A. Baikov, K.G. Chetyrkin, The structure of generic anomalous dimensions and no-π theorem for massless propagators, J. High Energy Phys. 06 (2018) 141, arXiv:1804.10088.
[46] J. Davies, A. Vogt, Absence of π^2 terms in physical anomalous dimensions in DIS: verification and resulting predictions, Phys. Lett. B 776 (2018) 189–194, arXiv:1711.05267.
[47] S. Catani, F. Hautmann, High-energy factorization and small x deep inelastic scattering beyond leading order, Nucl. Phys. B 427 (1994) 475–524, arXiv:hep-ph/9405388.
[48] J. Davies, C.H. Kom, S. Moch, A. Vogt, Resummation of small-x double logarithms in QCD: inclusive deep-inelastic scattering, J. High Energy Phys. 08 (2022) 135, arXiv:2202.10362.
[49] G. Soar, S. Moch, J.A.M. Vermaseren, A. Vogt, On Higgs-exchange DIS, physical evolution kernels and fourth-order splitting functions at large x, Nucl. Phys. B 832 (2010) 152–227, arXiv:0912.0369.